ON01910, a non-ATP-competitive small molecule inhibitor of Plk1, is a potent anticancer agent

Kiranmai Gumireddy,[1,3] M.V. Ramana Reddy,[1,3] Stephen C. Cosenza,[1,3] R. Boomi Nathan,[1] Stacey J. Baker,[1] Nabisa Papathi,[1] Jiandong Jiang,[2] James Holland,[2] and E. Premkumar Reddy[1,*]

[1]Fels Institute for Cancer Research and Molecular Biology, Temple University School of Medicine, 3307 N. Broad Street, Philadelphia, Pennsylvania 19140
[2]Department of Medicine, Mount Sinai School of Medicine, One Gustave L. Levy Place, New York, New York 10029
[3]These authors have contributed equally to this work
*Correspondence: reddy@temple.edu

Summary

Elevated expression of polo-like kinase1 (Plk1) has been reported in many human tumors, and inhibition of Plk1 activity results in their mitotic arrest and apoptosis. Here we describe the profile of ON01910, a small molecule inhibitor of Plk1 activity, which induces mitotic arrest of tumor cells characterized by spindle abnormalities leading to their apoptosis. This compound was not ATP-competitive, but competed for the substrate binding site of the enzyme. In vivo, this compound did not exhibit hematotoxicity, liver damage, or neurotoxicity, and was a potent inhibitor of tumor growth in a variety of xenograft nude mouse models. ON01910 showed strong synergy with several chemotherapeutic agents, often inducing complete regression of tumors.

Introduction

Cell cycle progression is orchestrated by Cyclin/CDK complexes, which are formed at specific stages of the cell cycle, and whose activities are required for progression through S phase and mitosis (Malumbres and Barbacid, 2001; Sherr and McCormick, 2002; Blagosklonny and Pardee, 2003). In addition to CDKs, several other families of protein kinases play a critical role in cell cycle progression. These include Aurora kinases, the NIMA family of kinases, the Mps1 gene product, and the Polo family of protein kinases (Reviewed in Hinchcliffe and Sluder, 2001).

The first member of the Plk gene family, POLO, was identified in *Drosophila melanogaster* and is a serine/threonine kinase required for mitosis (Fenton and Glover, 1993; Glover, 2005). Following the discovery of POLO, members of this gene family were identified in yeast, *C. elegans, Xenopus laevis,* mouse, and human (Kitada et al., 1993; Ohkura et al., 1995; Ouyang et al., 1999; Chase et al., 2002; Kumagai and Dunphy, 1996; Duncan et al., 2001; Donohue et al., 1995; Lake and Jelinek, 1993; Simmons et al., 1992; Hamanaka et al., 1995; Li et al., 1996). Members of this protein family are characterized by the presence of a conserved C-terminal domain, termed the POLO box, in addition to the kinase domain. Mutations in the Polo gene result in abnormal mitotic and meiotic division, and loss of its function has been shown to cause mitotic arrest (Fenton and Glover, 1993; Nigg, 1998).

Mammalian cells contain at least four members of this family, termed Plk1, Plk2 (also known as Snk), Plk3 (also known as Prk/Fnk), and Plk4 (also known as Sak) (Donohue et al., 1995; Hamanaka et al., 1995; Simmons et al., 1992; Fode et al., 1994). Of these, Plk1 has been the most extensively studied member of the family and is important for numerous aspects of mitotic progression, including centrosome maturation (Lane and Nigg, 1996), proper assembly of mitotic spindle (Sunkel and Glover, 1988), and activation of the anaphase promoting complex (Kotani et al., 1998). Ectopic overexpression of Plk1 in NIH/3T3 cells results in their transformation (Smith et al., 1997), and Plk1 mRNA and protein are overexpressed in many tumor cells, including breast, ovarian, non-small cell lung, head/neck, colon, endometrial and esophageal carcinomas, and leukemias, as well as carcinogen-induced rat tumors (Wolf et al., 1997; Knecht et al., 1999; Tokumitsu et al., 1999; Knecht et al., 2000; Strebhardt et al., 2000; Takai et al., 2001). More importantly, it has been shown that patients with esophageal carcinoma with a high level of Plk1 expression have a significantly poorer rate of survival than those with low levels of Plk1 expression (Knecht et al., 1999). In addition, it has been shown that downregulation of Plk1 activity using antibodies (Kotani et al., 1998), dominant negative mutants (Cogswell et al., 2000),

SIGNIFICANCE

Plk1, which is important for cell cycle progression through mitosis, is overexpressed in many tumor cells. Patients with high levels of Plk1 expression in their tumors were found to have a significantly poorer rate of survival than those with low levels of Plk1. Downregulation of Plk1 activity in tumor cells results in mitotic arrest characterized by spindle abnormalities and apoptosis. This report describes the antitumor activity of a small molecule inhibitor of Plk1, ON01910, and presents preclinical evidence of its low toxicity and efficacy in animal tumor models, both as a single agent and in synergistic combination with other chemotherapeutic agents. Based on the very desirable therapeutic index, ON01910 has entered Phase I clinical trials for cancer therapy.

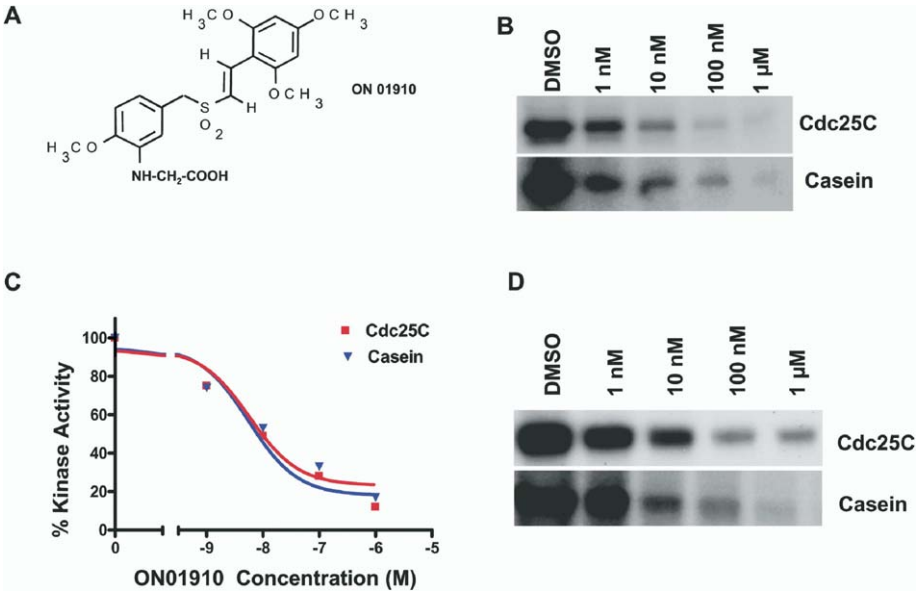

Figure 1. Identification of novel small molecule Plk1 inhibitor

A: Structure of the Plk1 inhibitor ON01910.

B: Plk1 inhibitory activity of ON01910. Ten nanograms of recombinant Plk1 was mixed with different concentrations of ON01910 and kinase assays performed as described in the Experimental Procedures using recombinant Cdc25C or casein as substrates. The reaction mixtures were subjected to SDS-PAGE and autoradiography.

C: Plk1 assays were performed as described in **B**, and the reactions spotted onto strips of P81 phosphocellulose paper, washed, and counted. The values from individual samples were analyzed and plotted as a function of drug concentration using Prism 4 Graphpad software.

D: Inhibition of mammalian Plk1 activity by ON01910. A synchronized population of HeLa cells at the midmitotic phase was used for the preparation of cell lysates and Plk1 immunoprecipitated from the clarified cell lysates as described in the Experimental Procedures. The precipitates were washed and the kinase assays performed in the presence of increasing concentrations of ON01910 as described in **B** using recombinant Cdc25C or casein as substrates.

anti-sense oligonucleotides (Spankuch-Schmitt et al., 2002b), or small interfering RNAs (Spankuch-Schmitt et al., 2002a, Liu and Erikson, 2003) results in mitotic arrest characterized by spindle abnormalities and apoptosis. In contrast to Plk1, other members of this family, such as Plk3, appear to function as growth suppressor genes (Dai and Cogswell, 2003; Conn et al., 2000), as suggested by their lack of expression in tumor tissues (Dai and Cogswell, 2003). Consistent with its role as a growth suppressor gene, ectopic overexpression of Plk3, but not that of a kinase-defective mutant, caused growth arrest and apoptosis of normal fibroblasts (Dai and Cogswell, 2003).

Here, we describe the profile of ON01910, a small molecule inhibitor of Plk1 that induces mitotic arrest in a wide range of tumor cells, characterized by spindle abnormalities leading to apoptotic death. This compound, which exhibits very little or no toxicity, was found to be a potent inhibitor of tumor growth in several animal models, and showed a high degree of synergism with several chemotherapeutic agents currently used in cancer therapy, often inducing complete regression of tumors.

Results

Derivation of a small molecule inhibitor of Plk1

We have recently described the synthesis of a family of novel small molecule kinase inhibitors that are unrelated to ATP (Reddy and Reddy, 2002a; Reddy and Reddy, 2002b; Reddy and Reddy, 2003) or other purine and pyrimidine nucleosides, and which exhibit potent antitumor activity. Screening of this novel library of molecules for antitumor activity using cell biological assays yielded several candidate molecules that appeared to induce mitotic arrest of tumor cells. Further analysis of these selected group of molecules for inhibitors of Plk1 activity led to the identification of one compound, ON01910 (Figure 1A), that had the most potent inhibitory activity. For these assays, 10 ng of recombinant Plk1 was mixed with different concentrations of ON01910 or DMSO (control) and kinase assays performed using Casein or Cdc25C as substrates. SDS-PAGE analysis of the reaction mixture showed that ON01910 is a potent inhibitor of Plk1 (Figure 1B). To determine the IC_{50} values, Plk1 assays were performed as described above, and the reaction mixture spotted onto strips of P81 phosphocellulose paper, washed, and counted. The values from individual samples were analyzed and plotted as a function of inhibitor concentration using Prism 4 Graphpad software for Macintosh. These studies revealed that ON01910 inhibits Plk1 with an IC_{50} of 9–10 nM. To ascertain that this inhibition was not restricted to recombinant Plk1, we examined the effects of ON01910 on the enzyme activity of Plk1 immunoprecipitated from a synchronized population of HeLa cells at midmitotic phase. Kinase assays performed with these immunoprecipitates (Figure 1D) again showed that ON01910 is a potent inhibitor of HeLa cell-derived Plk1, and the degree of inhibition seen with this preparation was similar to that seen with recombinant Plk1. It is interesting to note that when Cdc25C was used in these assays as a substrate, a residual level of phosphorylation was seen even in the presence of 1 μM ON01910, suggesting the existence of a residual level of kinase activity in the immunoprecipitates that is insensitive to ON01910. This may be due to contaminating kinases such as Chk1/2, which are known to interact with Plk1 and are capable of phosphorylating Cdc25C. We could also demonstrate the inhibition of Plk1 by ON01910 using a commercially available ELISA-based assay kit, the results of which are presented in Supplemental Figure S1.

Steady-state kinetic analysis of Plk1 inhibition by ON01910

To define the biochemical mechanism of action of ON01910, we examined the effects of increasing concentrations of ATP or substrate on the inhibitory activity of the compound using steady-state analysis. Ten nanograms of recombinant Plk1 was mixed with different concentrations of ON01910 and incubated at room temperature, followed by the addition of a reaction

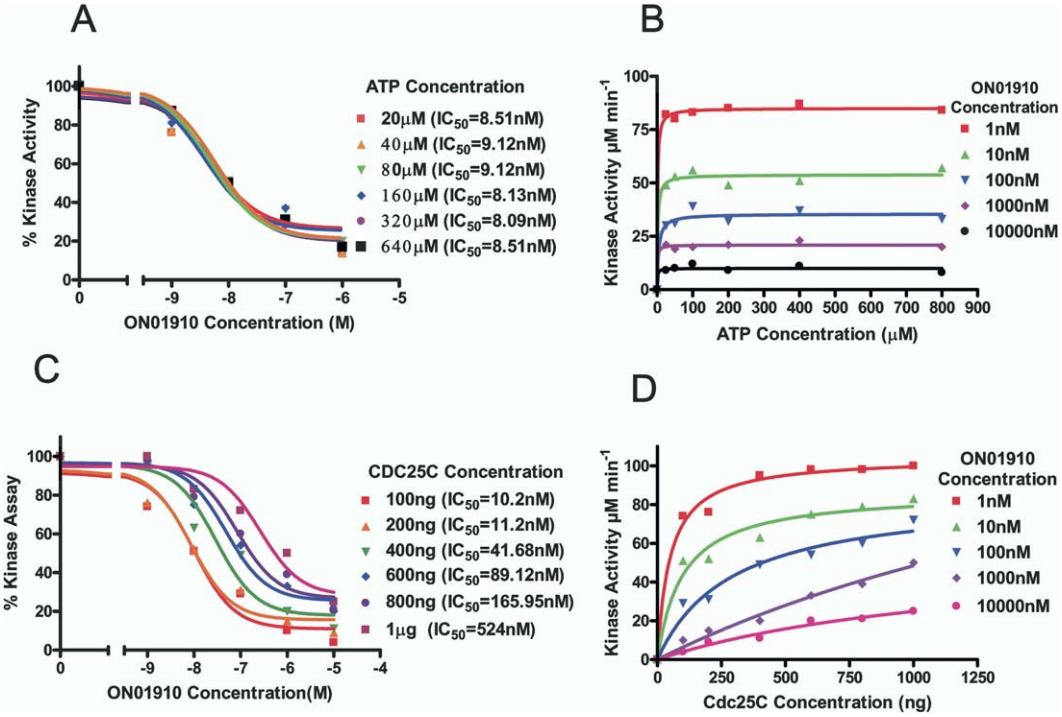

Figure 2. Steady-state kinetic analysis of PLK1 inhibition by ON01910

A: Ten nanograms of recombinant Plk1 was mixed with different concentrations of ON01910 and kinase assays performed in the presence of varying concentrations of ATP as described in Figure 1C. The values from individual samples were analyzed and plotted as a function of inhibitor concentration using Prism 4 Graphpad software.

B: Representative Michaelis-Menton curves with curve fit derived by nonlinear regression are shown.

C and D: IC_{50} curves (**C**) and Michaelis-Menton curves (**D**) for Plk1 in the presence of varying concentrations of Cdc25C substrate and ON01910 were generated as described in **A** and **B**.

mixture containing γ^{32}P-ATP and varying concentrations of ATP. Following termination of the reaction, the reaction mixture was spotted onto phosphocellulose strips, which were washed and counted. The values from individual samples were analyzed and plotted as a function of inhibitor concentration using Prism 4 Graphpad software (Figure 2A), and values for K_m (1.988 μM) and V_{max} (76.72 μM/min/mg protein) were obtained by fitting the data to the Michaelis-Menton equation (Cleland, 1977) (Figure 2B). These analyses showed that the velocity of substrate phosphorylation was unaltered in the presence of increasing concentrations of ATP, and the IC_{50} values for the inhibitor remained between 9 and 10 nM, suggesting that ON01910 is not an ATP-competitive inhibitor. We next examined the effects of increasing concentrations of substrate on the inhibitory activity of the compound in the presence of a constant amount of ATP (100 μM). Our studies (Figures 2C and 2D) showed that increasing the concentration of the substrate resulted in increased substrate phosphorylation in the presence of the inhibitor. Data analysis using the Michaelis-Menton equation (Cleland, 1977) demonstrated that the maximal velocity of Plk1 was not significantly affected by the inhibitor, while the apparent values for K_m were significantly increased. The increase in K_m, combined with unchanged V_{max} in the presence of an inhibitor, is characteristic of competitive inhibition. The IC_{50} values for the inhibition of Plk1 enzyme activity (Figures 2A–2D) demonstrate the substrate-dependent and ATP-independent nature of inhibition.

We next examined the inhibitory effects of ON01910 on a panel of serine/threonine and tyrosine kinases. These studies showed that at slightly higher concentrations, ON01910 exhibits inhibitory activity against three other kinases tested, the PDGF receptor (PDGFR), Abl, and Flt-1. At 10- to 20-fold higher concentrations, we also observed inhibition of CDK1, Plk2, Src, and Fyn (Supplemental Table S1). These results suggest a common feature shared between these kinases in their substrate binding sites. Of these different kinases, ON01910 was most active against Plk1, which is likely to be its primary target.

In vivo effects of ON01910 on Plk1 activity

Because inhibition of Plk1 synthesis or activity induced tumor cell death preceded by mitotic catastrophe (Reviewed in Dai and Cogswell, 2003), it was of interest to test the effect of ON01910 on the cell cycle progression, growth, and viability of human tumor cells. We tested the activity of ON01910 against 94 different tumor cell lines, and interestingly, this compound was found to induce apoptosis of all of these cell lines with a GI_{50} that ranged between 50–200 nM. (Selected data is shown in Table 1.) This compound was also tested by the National Cancer Institute, through its Developmental Therapeutics Program (DTP), against their panel of 57 human cancer cell lines (Grever et al., 1992). Their results showed that ON01910 had a broad-spectrum activity and inhibited the growth of all of the tested cell lines, including drug-resistant (MDR) cell lines, at nanomolar concentrations (data not shown). To further investi-

Table 1. In vitro tumor cell killing activity of ON01910

Tumor cell line	Tumor type	IC_{50} (nM)
BT20	Breast (ER–)	80
MCF-7	Breast (ER+)	50
T47D	Breast (ER+)	170
DU145	Prostate (AR–)	200
PC-3	Prostate (AR+)	150
MIA-PaCa2	Pancreatic	150
U87	Glioblastoma	80
H157	NSCLC	80
A549	NSCLC	90
H187	SCLC	80
N417	SCLC	80
AGS	Gastric	100
RF1	Gastric	50
RF48	Gastric	50
COLO-205	Colorectal	250
DLD-1	Colorectal	150
HCT15	Colorectal	125
SW480	Colorectal	170
Bel-7402	Hepatoma	100
DND-1A	Melanoma	75
KB	Nasopharyngeal	70
Drug-resistant cell lines and their normal counterparts		
MES-SA	Sarcoma	100
MES-SA/DX5	Resistant sarcoma	100
CEM	Leukemic	100
CEM/C2	Resistant leukemic	50
Normal cell lines		
HFL	Fibroblastic	>10,000
PrEC	Prostate epithelial	>10,000
HMEC	Mammary epithelial	>5,000
HUVEC	Umbilical vein endothelial	>10,000

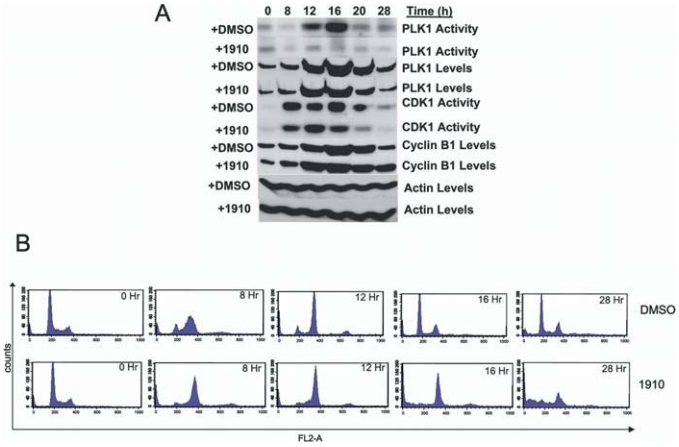

Figure 3. Effect of ON01910 on Plk1 activity and cell cycle progression of HeLa cells

A: HeLa cells blocked at the G1/S interphase with aphidicolin were released from G1 arrest and treated with DMSO or ON01910 (250 nM) for 8, 12, 16, 20, or 28 hr. Following incubation with DMSO or ON01910, cells were pelleted, lysed, and used for immunoprecipitation of CDK1 and Plk1. The immunoprecipitates were used for the determination of Plk1 and CDK1 kinase activities. Total cell lysates were also subjected to direct Western blots to determine the steady-state levels of Plk1 and Cyclin B1 and actin. **B:** Aliquots of HeLa cells treated with DMSO or ON01910 as described in **A** were fixed, stained with propidium iodide, and analyzed for their DNA content by flow cytometry.

gate the activity of this compound against MDR-positive tumor types, we determined the IC_{50} values of ON01910 using two classical MDR-positive, multidrug-resistant cell lines, MES-SA/DX5 (Harker and Sikic, 1985) and CEM/C2 (Fujimori et al., 1995). MES-SA/DX5 has been shown to express high levels of P-glycoprotein and is resistant to a number of drugs, including doxorubicin, paclitaxel, vincristine, vinblastine, etoposide, mitoxantrone, dactinomycin, and daunorubucin. The activity of ON01910 was then compared to the activity of paclitaxel (MDR-sensitive drug). Our results showed that while the parental cell line was very sensitive to paclitaxel (IC_{50} of 4 nM), the MDR-positive subline was greater than 100-fold resistant (IC_{50} of 750 nM) to paclitaxel (data not shown). However, when the two cell lines were treated with ON01910, both the parental and the MDR-positive cell lines were equally sensitive to the cell killing activity of the compound (Table 1). ON01910 resistance to atypical multidrug resistant cells was also investigated using the leukemic cell line CEM and its MDR+ subline CEM/C2 (Fujimori et al., 1995), which is resistant to camptothecin, etoposide, dactinimycin, bleomycin, mitoxantrone, doxorubicin, and daunorubicin. Our results again showed that CEM/C2 was highly sensitive to ON01910, suggesting that this compound does not share any crossresistance to classical MDR and atypical MDR cell lines (Table 1).

In vivo inhibition of Plk1 activity by ON01910

Because Plk1 has been shown to be essential for progression through mitosis and cytokinesis of many tumor cell lines, it was of interest to examine the effects of ON01910 on these cells. We chose to carry out these studies with HeLa cells, as they have been used extensively by several investigators to study the role of Plk1 in cell cycle progression. HeLa cells synchronized at the G1/S boundary by incubation with aphidicolin were released from G1 arrest by the removal of aphidicolin and reincubation in fresh medium containing 10% FBS. Cells were treated with DMSO or ON01910 for 8 hr, 12 hr, 16 hr, 20 hr, and 28 hr following the release from G1 block and examined for Plk1 activity and cell cycle progression. Analysis of the immunoprecipitates revealed that Plk1 activity is low or undetectable in control cells released from the G1/S block. This activity increased with time and reached a peak between the 12 and 16 hr time points, and was downregulated by 20 hr (Figure 3A). Plk1 assays carried out with immunoprecipitates derived from cells treated with ON01910 showed (Figure 3A) that treatment of cells with this compound resulted in a drastic reduction of Plk1 activity at all stages of the cell cycle, indicating that this compound acts as potent inhibitor of Plk1 activity in vivo. Direct Western blot analysis of the cell lysates showed that the steady-state levels of Plk1 in both ON01910 and DMSO-treated cells were low at the 0 and 8 hr time points and reached peak levels between 12 and 16 hr, followed by gradual downregulation, suggesting that the loss of Plk1 activity in ON01910-treated cells is not due to degradation of Plk1 or inhibition of Plk1 synthesis. In DMSO-treated cells, cyclin B1 levels were upregulated between 12 and 16 hr, followed by rapid downregulation as the cells exited mitosis followed by the onset of cytokinesis (Figure 3A). In cells treated with ON01910, cyclin B1 levels accumulated between 12 and 16 hr and failed to be downregulated, suggesting a block in mitotic progression and cytokinesis. The slightly lower levels of cyclin

B1 seen at the 28 hr time point appear to be due to the onset of apoptotic death in these cells. Measurement of CDK1 activity in control and 1910-treated cells revealed that like Plk1 activity, CDK1 activity was low in cells released from the aphidicolin block, increased with time, reached a peak around the 16 hr time point, and was downregulated by the 20 hr time point. ON01910-treated cells exhibited a slightly lower level of CDK1 activity, suggesting that this compound inhibits CDK1 activity, albeit with much lower potency than Plk1.

Effect of ON01910 on cell cycle progression of human tumor cells

Flow cytometric analysis of HeLa cells (Figure 3B) from the above set of experiments showed that control cells released from the aphidicolin block synchronously transited through S phase and entered the G2/M phase between the 12 and 16 hr time points. This was followed by cytokinesis and reentry of cells into the G1 phase between the 16 hr and 20 hr time points. It is interesting to note that Plk1 levels persist in cells that have gone through cytokinesis, consistent with previously published observations (Golsteyn et al., 1994). Incubation of HeLa cells with ON01910 following release from the aphidicolin block resulted in the accumulation of cells in the G2/M phase of the cell cycle between 8 and 16 hr, followed by rapid loss of viability. These results strongly suggest that ON01910-mediated mitotic arrest leads to tumor cell death.

We next investigated the effect of ON01910 on several normal human cell lines, which included fibroblastic cells as well as epithelial cell lines. Interestingly, these cell lines were found to be very resistant to the apoptotic effects of ON01910, which induced cell death only at 5–10 μM concentration (Table 1 and Supplemental Figure S2). When human fibloblastic cells (HFLs) were subjected to cell cycle analysis, both control and ON01910-treated cells progressed through mitosis without any abnormality, suggesting that ON01910 fails to block their cell cycle progression (Supplemental Figure S2B). It is interesting to note that previous studies using anti-sense oligonucleotides and small interfering RNAs directed against PLK1 showed that these agents, while readily blocking tumor cell cycle progression, failed to block cell cycle progression of normal fibroblasts and epithelial cell lines (Spankuch-Schmitt et al., 2002b). These results suggest the possibility that inhibition of PLK1 activity is more detrimental to tumor cells than normal cells. This could be due to the compensatory effects of other Plk family members in normal cells, a process that might be inoperative in tumor cells.

Effect of ON01910 on spindle assembly and cytokinesis

Plk1 is now known to be concentrated at the centrosomal region during interphase, and as cell cycle progression occurs, it associates with mitotic spindle poles. From metaphase onward, Plk1 relocates to the midzone, from which the midbody is eventually derived, as the cell goes through telophase (Glover et al., 1996; Wianny et al., 1998; Glover et al., 1998; Barr et al., 2004). Plk1-depleted HeLa cells were found to enter mitosis, but accumulated in a preanaphase state characterized by spindles that lacked focused poles and were not attached to centrosomes (Sumara et al., 2004). The chromosomes themselves also did not become stably attached to the spindle (Sumara et al., 2004). To test whether ON01910 induces spindle abnormalities, we examined the spindle architecture using confocal microscopy. HeLa cells blocked at the G1/S interphase with aphidicolin were released from G1 arrest, treated with DMSO or ON01910 (250 nM) for 7 or 12 hr, fixed with 4% paraformaldehyde, and treated with FITC-conjugated anti-α-tubulin antibody (to visualize tubulin spindles) and propidium iodide (to visualize chromosomal DNA). Confocal laser microscopy of the stained cells (Figure 4A) showed that while DMSO-treated cells go through various phases of mitosis without any abnormality, ON01910-treated cells exhibit profound abnormalities in spindle formation, resulting in the appearance of multipolar spindles, which leads to misalignment of chromosomes and complete loss of coordination in mitotic spindle assembly. In ON01910-treated cells, the chromosomes do not seem to be stably attached to the spindle, similar to the phenotype observed with Plk1-depleted cells (Sumara et al., 2004).

It is now known that Plk1 localizes to centrosomes during interphase and participates in microtubule dynamics. Plk1-depleted HeLa cells show abnormal localization of γ-tubulin, with centrosomes often depleted of γ-tubulin (Sumara et al., 2004). To determine the effects of ON01910 on centrosome dynamics, HeLa cells incubated with DMSO or ON01910 for 7 or 12 hr (as described above) were stained with antibodies to γ-tubulin and propidium iodide. As expected, in control cells, γ-tubulin antibodies stained centrosomes that formed the center of the spindle poles, which could be visualized at the 7 hr and 12 hr time points following the release from the aphidicolin block (Figure 4B). In sharp contrast, in cells treated with ON01910, these antibodies stained multiple centriole pairs, which seem to be randomly distributed in the area of the spindle, or even outside of it. Following a 12 hr incubation in the presence ON01910, degradation of these γ-tublin-positive structures could be readily visualized (Figure 4B). These observations suggest that exposure of tumor cells to ON01910 results in abnormal centrosome localization and fragmentation, which could be due to Plk1 inhibition.

A consequence of the mitotic abnormalities induced by this agent could be the activation of apoptotic pathways in ON01910-treated cells. To verify this possibility, HeLa cells treated with DMSO or ON01910 for 0, 24, and 48 hr were subjected to annexin V and propidium iodide staining followed by flow cytometric analysis. As can be seen in Figure 5A, DMSO-treated cells remain double-negative and hence viable at the 24 and 48 hr time points. On the other hand, cells treated with ON01910 become annexin V-positive within 24 hr and become double-positive within 48 hr of incubation, suggesting a rapid onset of apoptosis in these cells. The activation of apoptotic pathways could also be demonstrated by examining PARP (Poly[ADP-ribose] polymerase-1) cleavage (Soldani and Scovassi, 2002), which is a marker for caspase activation. Western blot analysis of HeLa cell lysates treated with DMSO or ON01910 (Figure 5B) show PARP cleavage in ON01910-treated cells as early as 24 hr, which becomes very pronounced by 48 hr, indicating the progression of apoptosis in these cells. Analysis of cell lysates for Caspase-3 activity also revealed a dramatic upregulation of this activity in ON01910-treated cells (Figure 5C).

To rule out the possibility that the chromosomal abnormalities induced by ON01910 are due to direct binding to β-tubulins and thereby interfering with its polymerization or depolymerization, we conducted in vitro polymerization reactions using ON01910. In these studies, paclitaxel, which stabilizes tubulin

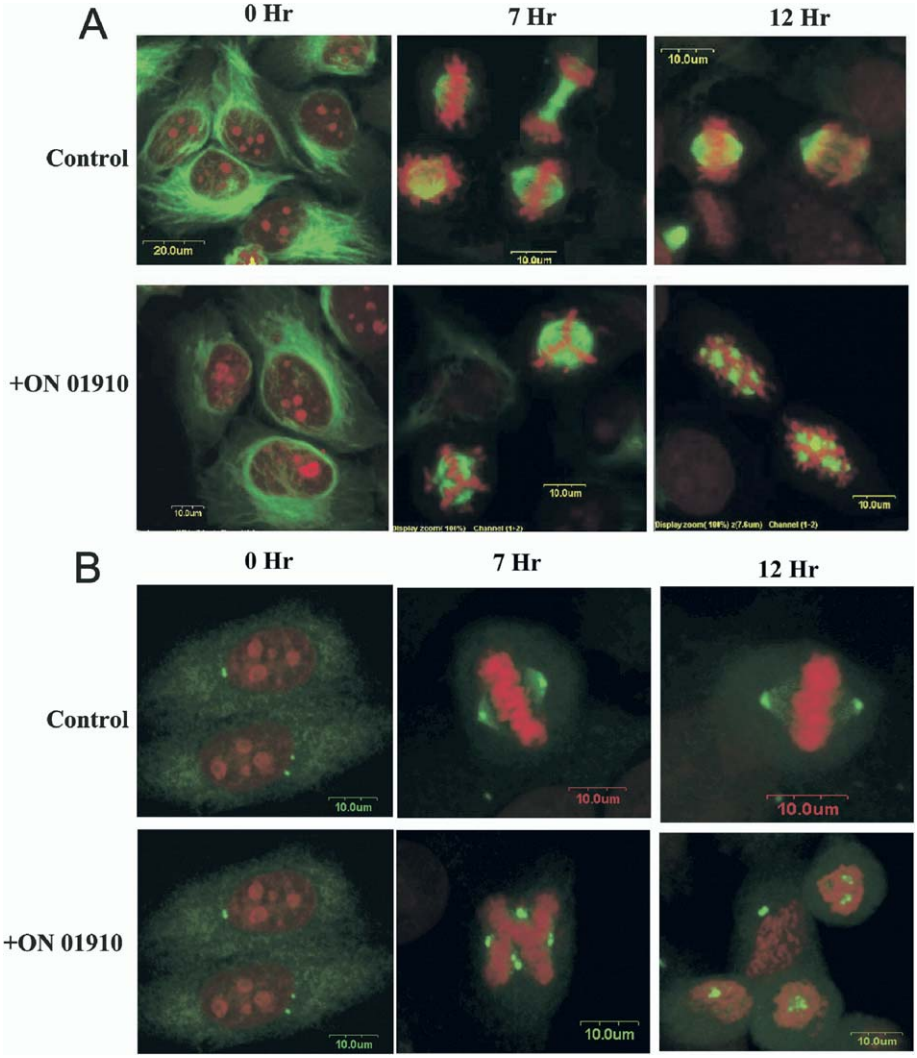

Figure 4. Induction of spindle abnormalities by ON01910 in human tumor cells

A: HeLa cells blocked at the G1/S interphase with aphidicolin were released from G1 arrest and treated with DMSO or ON01910 (250 nM) for 7 or 12 hr, fixed with 4% paraformaldehyde, and treated with an anti-α-tubulin antibody (FITC conjugated) and propidium iodide. The cells were analyzed by confocal laser microscopy.

B: Cells treated with anti-γ-tubulin antibody and propidium iodide.

polymerization, and vinblastine, which induces tubulin depolymerization, were used as controls. For these assays, purified bovine tubulin was incubated with GTP at 37°C in the presence of DMSO or different compounds dissolved in DMSO, and tubulin polymerization was detected by measuring the absorbance of the solution at 340 nm over time. The results of this study (Figure 5D) show that ON01910 had no effect on the kinetics of tubulin polymerization, while the addition of vinblastine inhibited tubulin polymerization and paclitaxel enhanced the polymerization.

Safety pharmacology

The safety profile of ON01910 was determined in two standard toxicology animal studies using rats and dogs (Table 2). In rats, single doses of 300 and 600 mg/m^2 produced no toxicity, and 1200 mg/m^2 had only slight toxicity (anogenital staining). When the dose was increased to 3000 mg/m^2, 9 of 11 animals died. In 7 day repeat dosing (1200 mg/m^2), 2 of 13 rats died during the dosing period. In 28 day repeat dosing, using groups of 12 male and 12 female rats, fixed daily doses of 180 mg/m^2 and 450 mg/m^2 were tolerated. A dose of 900 mg/m^2 given twice per week for 4 weeks was well tolerated. In dogs, acute single doses of 2000 and 4000 mg/m^2 produced gastrointestinal effects (diarrhea, flatulence), with other signs of discomfort during dosing at 4000 mg/m^2 (struggling, vocalization). In 7 day repeat i.v. dosing, 1000 mg/m^2 daily was well tolerated by dogs. In 28 day repeat dosing, daily intravenous doses of 200 and 500 mg/m^2 were well tolerated for 28 days in groups consisting of 3 male and 3 female beagle dogs. A high dose group started at 1000 mg/m^2 showed no signs of toxicity after 8 days. Based on dose escalation studies, a highest non-severe toxic dose for this dose schedule was estimated at about 1500 to 2000 mg/m^2 for 28 days. A separate group of 6 dogs treated at 1000 mg/m^2 twice per week for 4 weeks tolerated the compound well without clinical problems. There was no evidence of significant myelotoxicity, neuropathy, or cardiotoxicity in these toxicology studies.

Effects of ON01910 on tumor growth in nude mice

We next tested the in vivo antitumor activity of ON01910 using the nude mouse model system. Female athymic (NCr-nu/nu) mice were injected subcutaneously with 1 × 10^7 Bel-7402,

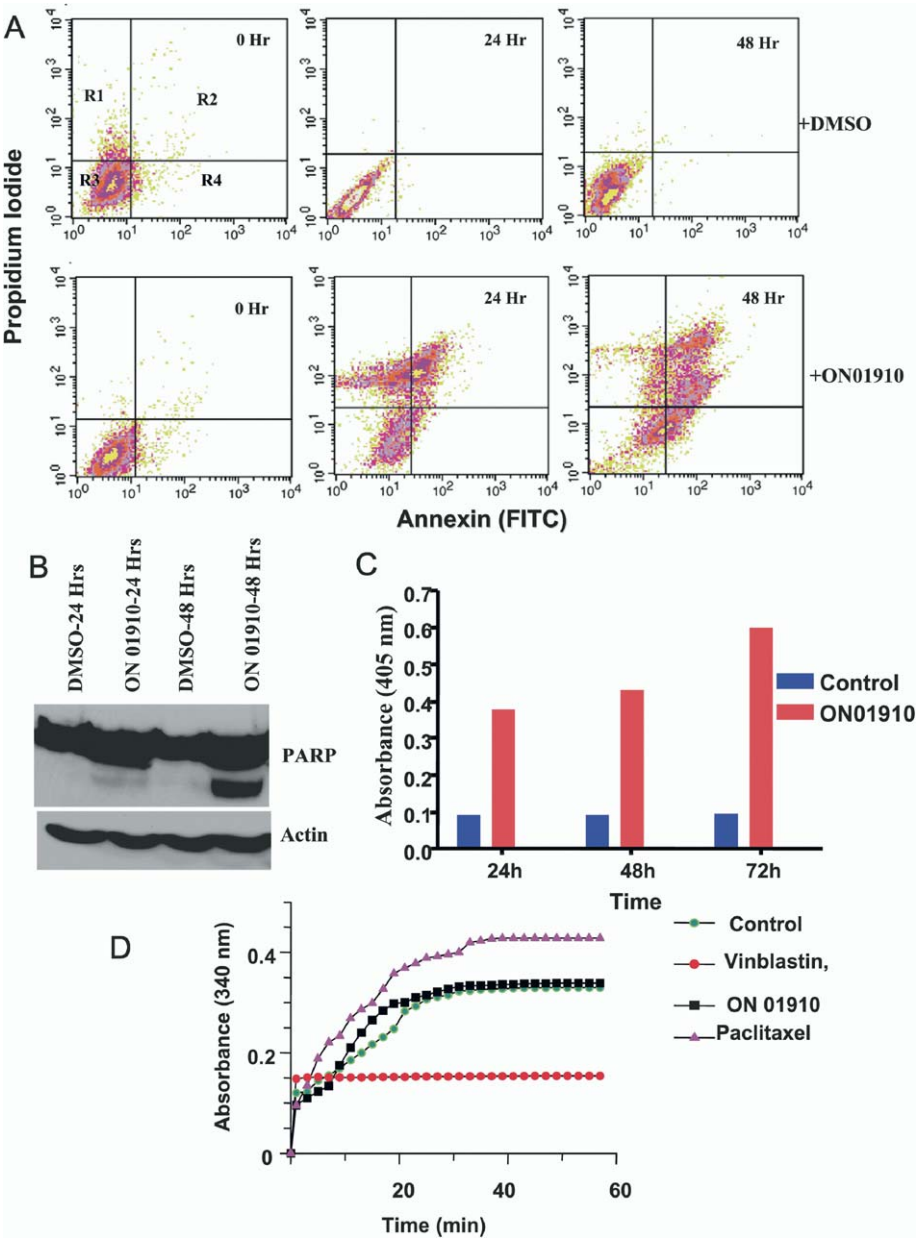

Figure 5. Induction of apoptosis by ON01910

A: HeLa cells treated with DMSO or ON01910 for 0, 24, and 48 hr were stained using FITC-conjugated Annexin V and propidium iodide and subjected to flow cytometric analysis as described in the Experimental Procedures. R1, Annexin-negative and PI-positive dead cells; R2, double-positive late apoptotic cells; R3, double-negative live cells; R4, Annexin V-positive, PI-negative early apoptotic cells.

B: Western blot analysis of cell lysates treated with DMSO or ON01910 using anti-PARP antibodies to assess the cleavage of PARP.

C: Levels of caspase-3 activity in DMSO and ON01910-treated HeLa Cells. HeLa cells (10^6 cells/ml) were treated with 100 nM ON01910 for 24, 48, and 72 hr. The level of caspase-3 activity was measured according to the assay conditions described in the Experimental Procedures.

D: Effect of ON01910 on in vitro polymerization of bovine brain tubulin. In vitro polymerization of purified bovine brain in the presence of DMSO (control), 5 μM ON01910, 5 μM vinblastine, or 5 μM paclitaxel was assessed as described in the Experimental Procedures.

MCF-7, or MIA PaCa human tumor cells derived from human liver, breast, and pancreatic cancers, respectively, and the tumors allowed to grow for 7–10 days to a size of 200–250 mm. The mice were then divided into four groups, of which one group received a dose of the vehicle alone and a second group received a dose of ON01910. In the case of the Bel-7402 tumors, the third group received a dose of oxaliplatin and the fourth group a combination of ON01910 and oxaliplatin. The tumor size and total body weights were then measured weekly as described in the Experimental Procedures. In the case of MCF-7-derived tumors, doxorubicin was used instead of oxaliplatin. MIA PaCa-derived tumors were treated with ON01910 or gemcitabine or a combination of ON01910 and gemcitabine as described in Experimental Procedures, and tumor volumes and body weights determined every third day. The results presented in Figures 6A, 6C, and 6E show that ON01910 readily inhibited tumor growth in these xenograft model systems. In all three cases, ON01910 had a better effect than the three therapeutic agents used for comparison. More importantly, there was no evidence of toxicity as judged by body weights (Figures 6B, 6D, and 6F). Bone marrow colony assays from ON01910-treated animals showed no decrease in colony formation (data not shown). Most interestingly, treatment of tumor-bearing mice with a combination of ON01910 and oxaliplatin or doxorubicin resulted in complete disappearance of the tumor mass in these animals. Treatment with a combination of gemcitabine and ON01910 resulted in a substantial decrease in tumor mass. To further verify the activity of ON01910, the tumor masses from one control mouse (treated with PBS) and two experimental animals (treated with ON01910) were re-

Table 2. Safety pharmacology of ON01910

Species	Dose schedule IV bolus	MTD mg/m^2	STD/LD$_{10}$ mg/m^2	HNSTD mg/m^2
Rats	Single dose	>1200 (no deaths)	<3000 (9/11 died)	—
Rats	7 day repeat		1200 (2/13 died)	—
Rats	2× per week, 4 weeks		<2100 (5/9 died)	—
Rats	28 day repeat	450 (1/36 died)	<900 (11/36 died)	—
Rats	2×/week, 4 weeks	900 (1 of 24 died)		—
Dogs	Single dose	>4000		2000
Dogs	7 day repeat	>1000		>1000
Dogs	2× per week, 4 weeks	>1000		
Dogs	28 day repeat	>1000	2500	1500–2000

MTD, maximum tolerated dose; STD, severely toxic dose; LD$_{10}$, dose producing lethality in 10% of animals; HNSTD, highest non-severely toxic dose

moved at the end of 21 days of treatment and tumor extracts prepared and analyzed for Plk1 and CDK1/Cyclin B1 activities. The data presented in Figure 6G show that the control tumor cell lysates exhibit very robust Plk1 and CDK1 activities, while the tumor cell lysates derived from the ON01910-treated mice had little or no Plk1 activity. CDK1 activity in the ON01910-treated samples was reduced, but not completely eliminated. Direct Western blot analyses revealed that tumor extracts from both control and ON01910-treated animals had similar steady-state levels of these two proteins. The low toxicity profile and potent tumor inhibitory activity seen in nude mouse xenograft assays points to the potential value of ON01910 as a safe therapy for cancer.

Discussion

Recent strides made in our understanding of the molecular changes that accompany cell transformation have established that cancer is the result of alterations in multiple signal transduction pathways. Drugs such as imatinib (also known as Gleevec or STI571), an inhibitor of the BCR-ABL tyrosine kinase (Druker and Lydon, 2000), has been a great success. Such drugs have a very targeted application in the treatment of a specific form of cancer with a mutation that is unique to that cancer. In addition to BCR-ABL, imatinib has also been found to be a potent inhibitor of PDGF receptor (PDGFR) and c-Kit (reviewed in Druker and Lydon, 2000; Sawyers, 2004). This crossreactivity may reflect the close structural similarity in the ATP binding pockets of these different kinases, which has provided new applications for this drug in the treatment of cancers where abnormalities in PDGFR and c-Kit expression play a critical role (Sawyers, 2004).

Because all signaling pathways that have gone awry in a cancer cell ultimately affect cell cycle progression, an alternative approach for cancer therapy is to develop inhibitors that block the function of a critical molecule that is required by a tumor cell to complete cell division. One such molecule appears to be Plk1. Named after the *Drosophila* polo gene, which was identified through a recessive maternal effect lethal mutation, this gene family is highly conserved throughout evolution from yeast to man and plays a critical role in centrosome maturation, progression through mitosis, and the onset of cytokinesis (Golsteyn et al., 1994; Glover et al., 1996; Wianny et al., 1998; Glover et al., 1998; Barr et al., 2004; Dai and Cogswell, 2003). In human cells, it has been shown that Plk1 stimulates the centrosome's microtubule nucleating activity upon mitotic entry, and mutation or inhibition of Plk1 results in aberrations in mitotic spindle formation (Glover et al., 1998; Barr et al., 2004). Plk1-depleted cells enter mitosis, but accumulate in a preanaphase state replete with spindle abnormalities characterized by the absence of focused poles, and chromosomes that do not become stably attached to the spindle (Sumara et al., 2004). Plk1 also appears to facilitate recruitment of γ-tubulin and activation of Asp at the centrosome, which helps focus the microtubule ends and maintain their proximity to the centrosome (Glover et al., 1998; Barr et al., 2004). Plk1 is also known to activate certain functions of the anaphase-promoting complex (APC), which triggers the destruction of Cyclin B, allowing mitotic exit (Barr et al., 2004; Lane and Nigg, 1996; Kotani et al., 1998). The concept that Plk1 is a potential target for cancer therapy has been substantiated by the observations that suppression of Plk1 expression or activity by anti-sense oligonucleotides or siRNAs or dominant negative mutants induces programmed cell death in human tumors, which is often preceded by abnormal spindle formation (Lane and Nigg, 1996; Cogswell et al., 2000; Spankuch-Schmitt et al., 2002a; Spankuch-Schmitt et al., 2002b; Liu and Erikson, 2003; Sumara et al., 2004).

By developing small molecule inhibitors of Plk1 which target regions outside the ATP binding site, we may avoid one of the anticipated problems associated with kinase inhibitors, the development of drug resistance as a result of accumulating mutations in the ATP binding site of the kinase, as has been observed in patients undergoing treatment with imatinib (Sawyers, 2004). Because selection of highly conserved mutable residues in the ATP binding site appears to be relatively common for many kinases, it has been argued that substrate-competitive inhibitors might constitute better drug candidates (Levitzki, 2000). In addition, many of the kinase inhibitors that are ATP mimetics inhibit their enzyme targets at nanomolar concentrations, while requiring micromolar concentration for tumor cell growth inhibition, and this discrepancy may be related to the need to overcome millimolar concentrations of ATP known to exist inside the cell (Levitzki, 2000). The results presented in this study describe the identification of a novel pharmacophore, which inhibits Plk1 at a 9–10 nM concentration and is noncompetitive to ATP. It is likely that this compound binds to Plk1 at or near the substrate binding domain, since substrates of Plk1 compete for the inhibitory activity of ON01910. In addition to Plk1, ON01910 was also inhibitory to Abl, Flt-1, and

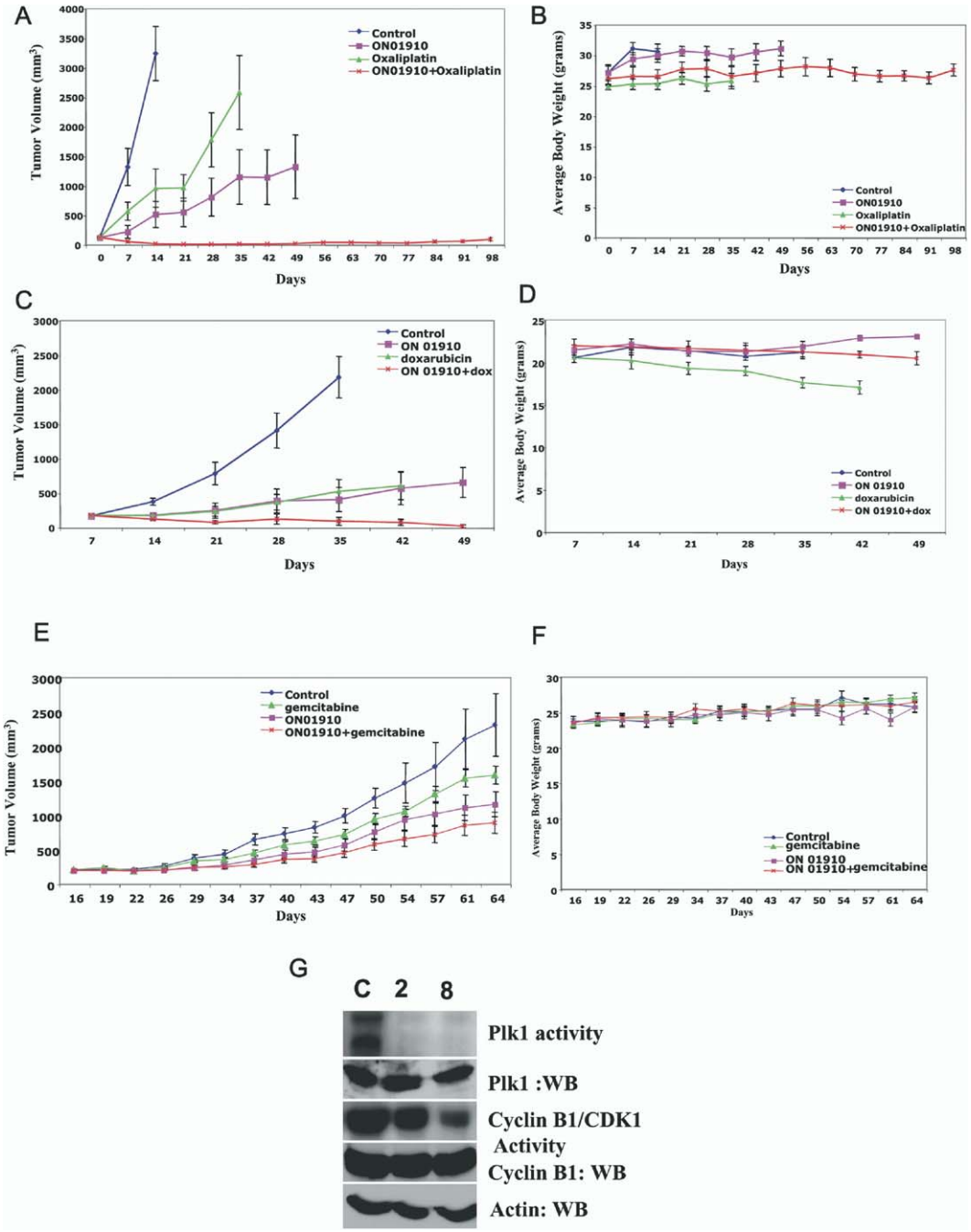

Figure 6. Antitumor activity of ON01910

A: Nude mouse xenograft assays using Bel-7402 human tumor cells was carried out using ON01910 or oxaliplatin or a combination of the two compounds, and tumor sizes measured weekly and the volume determined as described in the Experimental Procedures.

B: Total body weight of individual mice in the four groups was determined weekly and the average body weights plotted.

C: Nude mouse xenograft assays using MCF-7 human tumor cells using doxorubicin or ON01910 or a combination of the two compounds were carried out, and tumor sizes measured weekly and the volume determined as described in the Experimental Procedures.

D: Total body weight of individual mice in the four groups was determined weekly and the average body weights plotted.

E: Nude mouse xenograft assays using human pancreatic tumor cells MIA-PaCa was carried out using ON01910 or gemcitabine or a combination of the two compounds, and tumor sizes measured biweekly and the volume determined as described in the Experimental Procedures.

F: Total body weight of individual mice in the four groups was determined biweekly and the average body weights plotted. The data in **A**, **C**, and **E** represent average tumor volume ± SEM, and the data in **B**, **D** and **F** represent average body weight ± SEM

G: Tumors excised from one control mouse (lane C) and two experimental animals treated with ON01910 (lanes 2 and 8) were minced and homogenized in modified RIPA buffer (150 mM NaCl, 50 mM Tris-HCl [pH 7.4], 1 mM EDTA, 1 mM PMSF, 1% Triton X100, and a cocktail of protease inhibitors; Roche Applied Science, Indianapolis) and clarified by centrifugation at 13,000 × g for 15 min at 4°C. The supernatants were immunoprecipitated with antibodies directed against Plk1 or Cyclin B1 and the immunoprecipitates used to carry out kinase assays using casein or Histone H1 as substrates, as described in Figure 3. Direct Western blot analysis of the tumor lysates was performed using 50 μg of the total protein.

PDGFR kinases at low nanomolar concentrations. At approximately 10- to 20-fold higher concentrations, inhibition of Src, Fyn, and Plk2 kinases was also observed. While it is possible that inhibition of these kinases may play a role in the phenotype observed in ON01910-treated cells, the fact that this compound is most active against Plk1 suggests that this enzyme is the primary target of this compound.

ON01910 induces mitotic arrest in a wide variety of human tumor cells, characterized by spindle abnormalities leading to their apoptotic death. Most interestingly, MDR-positive cells, which are resistant to many commonly used chemotherapeutic agents, were nevertheless very sensitive to the activity of this compound. Because mutations in the ATP binding site appear to be relatively common for many kinases, we tested whether we could select for resistance to ON01910 in tumor cells by culturing them in the presence of sublethal amounts of the compound. In these experiments, we could isolate cell lines resistant to other chemotherapeutic drugs, but none of the cell lines exhibited increased survival to ON01910 (data not shown). These results suggest that mutations in the ON01910 binding site are difficult to generate. A possible explanation could be that such mutations lead to inactivation of the enzyme, which in turn results in the loss of tumor cell viability or loss of growth advantage.

Our in vitro studies with normal human cell lines (PrEC, HMEC, and HFL Cells) show that they are very resistant to the apoptotic effects of ON01910, which is in sharp contrast to the effects seen with tumor cell lines. This is also reflected in the very desirable safety profile that is not often seen in conventional chemotherapeutic agents. In rats, single doses of 300 and 600 mg/m² of ON01910 produced no toxicity, and 1200 mg/m² had only slight toxicity. There was no evidence of significant myelotoxicity, neuropathy, or cardiotoxicity in these toxicology studies. In xenograft mouse model systems, this compound inhibited the growth of a wide variety of human tumors, including liver, breast, and pancreatic cancers. More importantly, this compound was highly efficacious in combination with other chemotherapeutic agents such as oxaliplatin and doxorubicin, often resulting in complete remission of the tumors in xenograft model systems.

The low in vivo toxicity and the potent tumor inhibitory activity seen in nude mouse xenograft assays (i.e., a high therapeutic index) led to Phase I trials of ON01910, which are currently in progress. Because this compound is highly effective in various combinations with conventional chemotherapy, the lack of bone marrow toxicity may be beneficial for testing novel combinations for advanced cancers, including tumors resistant to conventional chemotherapy. Clinical studies, which are currently in progress, should reveal the best way to utilize ON01910 in human cancer therapy.

Experimental procedures

Cell culture and viability assays

ON01910 was synthesized in the laboratory, and its purity and structure were confirmed by HPLC, melting points, and NMR. Paclitaxel was purchased from Sigma. All cell lines were grown in DMEM or RPMI (Cellgro), supplemented with 10% fetal bovine serum (Atlas Co) and 1 unit/ml of penicillin-streptomycin. Cell viability assays were performed by incubation in the presence of the drug for 96 hr and the number of viable cells determined by trypan blue exclusion.

Analysis of cell cycle progression and apoptosis

HeLa cells were synchronized at the G1/S boundary by aphidicolin block as described by Heintz et al. (1983). Briefly, exponentially growing cells were treated with aphidicholin (1 μg/ml, Sigma) for 14 hr followed by washing thrice with normal growth medium and incubation in the presence or absence of ONO1910. At the indicated intervals, cells were collected by trypsinization, washed with PBS, fixed in 70% ethanol, incubated with propidium iodine (50 ug/ml) and RNase A (0.5 mg) for 30 min, and analyzed on a Becton-Dickinson (BD) (FACScan) flow cytometer. Staining with FITC-Annexin V was carried out as described by the manufacturer (BD Biosciences). PARP cleavage assays were performed with equal amounts of total cellular proteins that were resolved on a 10%-SDS-polyacrylamide gel, and Western blotting analysis performed using anti-PARP antibodies (BD Biosciences). Caspase 3 activity was measured using a commercial caspase-3 assay kit (CaspACE, Promega, Madison, WI). Caspase enzymatic hydrolysis was measured by pNA liberation from Ac-DEVD-pNA upon cleavage by DEVDase at 405 nm using a spectrophotometer.

Tubulin polymerization assays

Tubulin polymerization assays were performed using the Tubulin Polymerization Assay Kit (Cytoskeleton Inc., Denver, CO) according to the manufacturer's instructions. Tubulin polymerization was monitored by measuring the change in absorbance at 340 nm for 60 min at one minute intervals at 37°C in a Perkin Elmer HTS 7000 Plus Bioassay Reader.

Confocal microscopy

HeLa cells grown on glass coverslips were washed with PBS and fixed in 4% paraformaldehyde. The fixed cells were then treated with PBS containing 10% FBS/0.1% Triton X-100 for 45 min at room temperature followed by washing and incubation with monoclonal anti α-tubulin antibody or anti-γ tubulin antibody conjugated with FITC (DM1A, Sigma) for 1 hr at 37°C. The coverslips were washed, treated with propidium iodide (1 μg/ml in PBS) for 5 min, washed again, and mounted onto slides using prolong antifade solution (Molecular Probes). The stained cells were analyzed by using the inverted Olympus confocal microscope FluoView system with a 60× objective.

In vitro enzyme assays for Plk1

Plk1 expressed in the Sf9 cell line was purified as described by Lee and Erikson (1997). 10 ng of recombinant Plk1 was incubated with different concentrations of ON01910 in a 15 μl reaction mixture (50 mM HEPES, 10 mM $MgCl_2$, 1 mM EDTA, 2 mM Dithiothreitol, 0.01% NP-40 [pH 7.5]) for 30 min at room temperature. Kinase reactions were performed for 20 min at 30°C in a volume of 20 μl (15 μl enzyme + inhibitor, 2 μl 1 mM ATP), 2 μl of γ ^{32}PATP (40 μci), and 1 μl of recombinant Cdc25C (100 ng) or casein (1 μg) substrates. Reactions were terminated by boiling for 2 min in 20 μl of 2× Laemmli buffer (Laemmli, 1970). Phosphorylated substrates were separated by 18% SDS-PAGE (Laemmli, 1970). The gels were dried and exposed to X-ray film for 3–10 min.

Filter binding assays for Plk1

Plk1 assays were performed as above. After incubation, 10 μl aliquots of the reaction mixture were spotted onto a P81 phosphocellulose paper. The filters were washed 3 times for 5 min each with 0.75% phosphoric acid followed by acetone, and the radioactivity determined using a liquid scintillation counter. Control samples contained appropriate amounts of DMSO. Nonspecific binding was determined by conducting the assay in the absence of the enzyme, and the values subtracted from each of the experimental values. The kinase activity is expressed as a percent of the maximal kinase activity. Dose response curves were used for calculating IC_{50} values. All assays were carried out in triplicate.

In vitro assays for Plk1 and CDK1 using cell lysates

Cells were washed with PBS and lysed in lysis buffer (25 mm HEPES, 0.1% Triton-X-100, 300 mM NaCl, 0.5 mM DTT, 0.2 mM Na_3VO_4, 0.2 mm EDTA, 1.5 mM $MgCl_2$, 20 mm β-glycerophosphate and protease inhibitor cocktail). Following high-speed centrifugation, the cell lysates were used for various kinase assays. For CDK1 assays, 100 μg of total protein was incubated with 5 μg of anti-CDK1 or anti-cyclin B1, antibodies, and protein A agarose for 2 hr at 4°C. The protein complexes were washed three times with lysis

buffer and once with kinase buffer (50 mM HEPES, 10 mM $MgCl_2$, 1 mM EDTA, 2 mM Dithiothreitol 0.01% NP-40 [pH 7.5]). The kinase reactions were carried out at 30°C for 20 min in 20 µl of kinase reaction buffer containing 100 µM ATP, 40 µCi γ^{32}PATP, and 1 µg of Histone H1. The reaction was stopped by adding 2× Laemmli buffer and boiling for 5 min. The reaction products were separated by 12% SDS PAGE and phosphorylated proteins detected by autoradiography. For Plk1 assays, a similar protocol was used, using anti-Plk1 antibodies for immunoprecipitation and Cdc25C (100 ng) or casein (2 µg) as substrates.

Nude mouse assays

Bel-7402 tumor models: twenty female athymic (NCR-nu/nu, Tacomic) nude mice were injected with 1×10^7 Bel-7402 tumor cells subcutaneously, and 10–14 days later, when the tumor volumes reached 200–250 mm, the mice were divided into four groups such that each group harbored tumors of the same volume. ON01910 (250 mg/kg) dissolved in PBS was administered alone or in combination with oxaliplatin (100 mg/kg) intraperitonially on alternate days. Tumor measurements were done two times/week using traceable digital vernier calipers (Fisher). Body weight was determined during each measurement. The animals were observed for signs of toxicity.

MCF-7 tumor model: 1×10^7 MCF-7 breast tumor cells were injected subcutaneously and the tumors were allowed to grow to a size of 200–250 mm over a period of 10–15 days. For this breast tumor model system, estradiol pellets (1 mg) were implanted interscapularly 24 hr before tumor implantation in the mammary fat pad. When the tumor volumes reached 200–250 mm, the mice were divided into four groups and were treated with PBS alone or ON01910 (250 mg/kg) dissolved in PBS or with doxorubicin (2.5 mg/kg) or a combination of ON01910 (250 mg/kg) and doxorubicin (2.5 mg/kg) intraperitonially on alternate days. Tumor measurements (two dimensions) were performed as described for the Bel-7402 tumor system.

MIA-PaCa tumor model: Forty female athymic (NCR-nu/nu, Tacomic) nude mice were each injected with 1×10^7 MIA PaCa pancreatic tumor cells subcutaneously, and tumors were allowed to grow to a size of 200–250 mm over a period of 10–15 days. When the tumor volumes reached 200–250 mm, the mice were divided into four groups and were treated with PBS alone or ON01910 (250 mg/kg) dissolved in PBS or with gemcytabine (100 mg/kg) or a combination of ON01910 (250 mg/kg) and gemcytabine (100 mg/kg) intraperitonially on alternate days. Tumor measurements (two dimensions) were performed as described for the Bel-7402 tumor system. Tumor volume was calculated using the following equation: $V = Lx(S^2)\pi/6$, where L is the longer and S is the shorter of the two dimensions.

Supplemental data

Supplemental data for this article can be found at http://www.cancercell.org/cgi/content/full/7/3/275/DC1/.

Acknowledgments

We gratefully acknowledge the help of Dr. Raymond Erikson, who provided us with the sf9 cells expressing Plk1. This work was supported by grants from Onconova Therapeutics Inc. and the Fels Foundation. We thank Dr. Ramesh Kumar for helpful advice. This work was supported by a grant from Onconova Therapeutics Inc. drug discovery program, and E.P.R. and M.V.R.R. are stockholders of Onconova Therapeutics Inc. E.P.R., S.C.C., and M.V.R.R. are consultants to Onconova Therapeutics Inc.

Received: October 19, 2004
Revised: January 21, 2005
Accepted: February 22, 2005
Published: March 14, 2005

References

Barr, F.A., Sillje, H.H., and Nigg, E.A. (2004). Polo-like kinases and the orchestration of cell division. Nat. Rev. Mol. Cell Biol. *5*, 429–440.

Blagosklonny, M.V., and Pardee, A.B. (2003). The restriction point of the cell cycle. Cell Cycle *1*, 103–110.

Chase, D., Golden, A., Heidecker, G., and Ferris, D.K. (2002). Caenorhabditis elegans contains a third polo-like kinase gene. DNA Seq. *11*, 327–334.

Cleland, W.W. (1977). Determining the chemical mechanisms of enzyme-catalyzed reactions by kinetic studies. Adv. Enzymol. Relat. Areas Mol. Biol. *45*, 273–387.

Cogswell, J.P., Brown, C.E., Bisi, J.E., and Neill, S.D. (2000). Dominant-negative polo-like kinase 1 induces mitotic catastrophe independent of cdc25C function. Cell Growth Differ. *11*, 615–623.

Conn, C.W., Hennigan, R.F., Dai, W., Sanchez, Y., and Stambrook, P.J. (2000). Incomplete cytokinesis and induction of apoptosis by overexpression of the mammalian polo-like kinase, Plk3. Cancer Res. *60*, 6826–6831.

Dai, W., and Cogswell, J.P. (2003). Polo-like kinases and the microtubule organization center: targets for cancer therapies. Prog. Cell Cycle Res. *5*, 327–334.

Donohue, P.J., Alberts, G.F., Guo, Y., and Winkles, J.A. (1995). Identification by targeted differential display of an immediate early gene encoding a putative serine/threonine kinase. J. Biol. Chem. *270*, 10351–10357.

Druker, B.J., and Lydon, N.B. (2000). Lessons learned from the development of an abl tyrosine kinase inhibitor for chronic myelogenous leukemia. J. Clin. Invest. *105*, 3–7.

Duncan, P.I., Pollet, N., Niehrs, C., and Nigg, E.A. (2001). Cloning and characterization of Plx2 and Plx3, two additional Polo-like kinases from Xenopus laevis. Exp. Cell Res. *270*, 78–87.

Fenton, B., and Glover, D.M. (1993). A conserved mitotic kinase active at late anaphase-telophase in syncytial Drosophila embryos. Nature *363*, 637–640.

Fode, C., Motro, B., Yousefi, S., Heffernan, M., and Dennis, J.W. (1994). Sak, a murine protein-serine/threonine kinase that is related to the drosophila polo kinase and involved in cell proliferation. Proc. Natl. Acad. Sci. USA *91*, 6388–6392.

Fujimori, A., Harker, W.G., Kohlhagen, G., Hoki, Y., and Pommier, Y. (1995). Mutation at the catalytic site of topoisomerase I in CEM/C2, a human leukemia cell line reisitant to camptothecin. Cancer Res. *55*, 1339–1346.

Glover, D.M. (2005). Polo kinase and progression through M phase in Drosophila: a perspective from the spindle poles. Oncogene *24*, 292–298.

Glover, D.M., Ohkura, H., and Tavares, A. (1996). Polo kinase: the choreographer of the mitotic stage? J. Cell Biol. *135*, 1681–1684.

Glover, D.M., Hagan, I.M., and Tavares, A.A. (1998). Polo-like kinases: a team that plays throughout mitosis. Genes Dev. *12*, 3777–3787.

Golsteyn, R.M., Schultz, S.J., Bartek, J., Ziemiecki, A., Ried, T., and Nigg, E.A. (1994). Cell cycle analysis and chromosomal localization of human Plk1, a putative homologue of the mitotic kinases Drosophila polo and Saccharomyces cerevisiae Cdc5. J. Cell Sci. *107*, 1509–1517.

Grever, M.R., Schepartz, S.A., and Chabner, B.A. (1992). The National Cancer Institute: Cancer Drug Discovery and Development Program. Semin. Oncol. *19*, 622–663.

Hamanaka, R., Smith, M.R., O'Connor, P.M., Maloid, S., Mihalic, K., Spivak, J.L., Longo, D.L., and Ferris, D.K. (1995). Polo-like kinase is a cell cycle-regulated kinase activated during mitosis. J. Biol. Chem. *270*, 21086–21091.

Harker, W.G., and Sikic, B.I. (1985). Multidrug (pleiotropic) resistance in doxorubicin-selected variants of the human sarcoma cell line MES-SA. Cancer Res. *45*, 4091–4096.

Heintz, N., Sive, H.I., and Roeder, R.G. (1983). Regulation of human histone gene expression: kinetics of accumulation and changes in the rate of synthesis and in the half-lives of individual histone mRNAs during the HeLa cell cycle. Mol. Cell. Biol. *3*, 539–550.

Hinchcliffe, E.H., and Sluder, G. (2001). Centrosome duplication: three kinases come up a winner! Curr. Biol. *11*, R698–R701.

Kitada, K., Johnson, A.L., Johnston, L.H., and Sugino, A.A. (1993). Multicopy suppressor gene of the Saccharomyces cerevisiae G1 cell cycle mutant gene dbf4 encodes a protein kinase and is identified as CDC5. Mol. Cell. Biol. *13*, 4445–4457.

Knecht, R., Elez, R., Oechler, M., Solbach, C., von Ilberg, C., and Strebhardt, K. (1999). Prognostic significance of polo-like kinase (Plk) expression in squamous cell carcinomas of the head and neck. Cancer Res. *59*, 2794–2797.

Knecht, R., Oberhauser, C., and Strebhardt, K. (2000). Plk (polo-like kinase), a new prognostic marker for oropharyngeal carcinomas. Int. J. Cancer *89*, 535–536.

Kotani, S., Tugendreich, S., Fujii, M., Jorgensen, P.M., Watanabe, N., Hoog, C., Hieter, P., and Todokoro, K. (1998). PKA and MPF-activated polo-like kinase regulate anaphase-promoting complex activity and mitosis progression. Mol. Cell *1*, 371–380.

Kumagai, A., and Dunphy, W.G. (1996). Purification and molecular cloning of Plx1, a Cdc25-regulatory kinase from Xenopus egg extracts. Science *273*, 1377–1380.

Laemmli, U.K. (1970). Cleavage of structural proteins during the assembly of the head of bacteriophage T4. Nature *227*, 680–685.

Lake, R.J., and Jelinek, W.R. (1993). Cell cycle- and terminal differentiation-associated regulation of the mouse mRNA encoding a conserved mitotic protein kinase. Mol. Cell. Biol. *13*, 7793–7801.

Lane, H.A., and Nigg, E.A. (1996). Antibody microinjection reveals an essential role for human polo-like kinase 1 (Plk1) in the functional maturation of mitotic centrosomes. J. Cell Biol. *135*, 1701–1713.

Lee, K.S., and Erikson, R.L. (1997). Plk is a functional homolog of Saccharomyces cerevisiae Cdc25, and elevated Plk activity induces multiple septation structures. Mol. Cell. Biol. *17*, 3408–3417.

Levitzki, A. (2000). Protein tyrosine kinase inhibitors as therapeutic agents. Top. Curr. Chem. *211*, 1–15.

Li, B., Ouyang, B., Pan, H., Reissmann, P.T., Slamon, D.J., Arceci, R., Lu, L., and Dai, W. (1996). Prk, a cytokine-inducible human protein serine/threonine kinase whose expression appears to be down-regulated in lung carcinomas. J. Biol. Chem. *271*, 19402–19408.

Liu, X., and Erikson, R.L. (2003). Polo-like kinase (Plk)1 depletion induces apoptosis in cancer cells. Proc. Natl. Acad. Sci. USA *100*, 5789–5794.

Malumbres, M., and Barbacid, M. (2001). To cycle or not to cycle: a critical decision in cancer. Nat. Rev. Cancer *1*, 222–231.

Nigg, E.A. (1998). Polo-like kinases: Positive regulators of cell division from start to finish. Curr. Opin. Cell Biol. *10*, 776–783.

Ohkura, H., Hagan, I.M., and Glover, D.M. (1995). The conserved Schizosaccharomyces pombe kinase plo1, required to form a bipolar spindle, the actin ring, and septum, can drive septum formation in G1 and G2 cells. Genes Dev. *9*, 1059–1073.

Ouyang, B., Wang, Y., and Wei, D. (1999). Caenorhabditis elegans contains structural homologs of human prk and Plk. DNA Seq. *10*, 109–113.

Reddy, E.P., and Reddy, M.V.R. (2002a). Preparation of α,β-unsaturated sulfones for treating proliferative disorders. U.S. Patent No. 6541475.

Reddy, E.P., and Reddy, M.V.R. (2002b). Substituted styryl benzylsulfones for treating proliferative disorders. US Patent No. 6486210 B2.

Reddy, E.P., and Reddy, M.V.R. (2003). α,β-unsaturated sulfones for treating proliferative disorders. US Patent No. 6599932 B1.

Sawyers, C.L. (2004). Opportunities and challenges in the development of kinase inhibitor therapy for cancer. Genes Dev. *17*, 2998–3010.

Sherr, C.J., and McCormick, F. (2002). The Rb and p53 pathways in cancer. Cancer Cell *2*, 103–112.

Simmons, D.L., Neel, B.G., Stevens, R., Evett, G., and Erikson, R.L. (1992). Identification of an early-growth-response gene encoding a novel putative protein kinase. Mol. Cell. Biol. *12*, 4164–4169.

Smith, M.R., Wilson, M.L., Hamanaka, R., Chase, D., Kung, H., Longo, D.L., and Ferris, D.K. (1997). Malignant transformation of mammalian cells initiated by constitutive expression of the polo-like kinase. Biochem. Biophys. Res. Commun. *234*, 397–405.

Soldani, C., and Scovassi, A.I. (2002). Poly(ADP-ribose) polymerase-1 cleavage during apoptosis: an update. Apoptosis *7*, 321–328.

Spankuch-Schmitt, B., Bereiter-Hahn, J., Kaufmann, M., and Strebhardt, K. (2002a). Effect of RNA silencing of polo-like kinase-1 (Plk1) on apoptosis and spindle formation in human cancer cells. J. Natl. Cancer Inst. *94*, 1863–1877.

Spankuch-Schmitt, B., Wolf, G., Solbach, C., Loibl, S., Knecht, R., Stegmuller, M., von Minckwitz, G., Kaufmann, M., and Strebhardt, K. (2002b). Downregulation of human polo-like kinase activity by antisense oligonucleotides induces growth inhibition in cancer cells. Oncogene *21*, 3162–3171.

Strebhardt, K., Kneisel, L., Linhart, C., Bernd, A., and Kaufmann, R. (2000). Prognostic value of pololike kinase expression in melanomas. JAMA *283*, 479–480.

Sumara, I., Glimenez-Alban, J.F., Gerlich, D., Hirota, T., Kraft, C., de la Torre, C., Ellenberg, J., and Peters, J.-M. (2004). Roles of Polo-like kinase 1 in the assembly of functional mitotic spindles. Curr. Biol. *14*, 1712–1722.

Sunkel, C.E., and Glover, D.M. (1988). polo, a mitotic mutant of Drosophila displaying abnormal spindle poles. J. Cell Sci. *89*, 25–38.

Takai, N., Miyazaki, T., Fujisawa, K., Nasu, K., Hamanaka, R., and Miyakawa, I. (2001). Expression of polo-like kinase in ovarian cancer is associated with histological grade and clinical stage. Cancer Lett. *164*, 41–49.

Tokumitsu, Y., Mori, M., Tanaka, S., Akazawa, K., Nakano, S., and Niho, Y. (1999). Prognostic significance of polo-like kinase expression in esophageal carcinoma. Int. J. Oncol. *15*, 687–692.

Wianny, F., Tavares, A., Evans, M.J., Glover, D.M., and Zernicka-Goetz, M. (1998). Mouse polo-like kinase 1 associates with the acentriolar spindle poles, meiotic chromosomes and spindle midzone during oocyte maturation. Chromosoma *107*, 430–439.

Wolf, G., Elez, R., Doermer, A., Holtrich, U., Ackermann, H., Stutte, H.J., Altmannsberger, H.M., Rubsamen-Waigmann, H., and Strebhardt, K. (1997). Prognostic significance of polo-like kinase (Plk) expression in non-small cell lung cancer. Oncogene *14*, 543–554.